Chapter 4

Instabilities of a cylindrical vortex

Consider a cylindrical coordinate system with radial, azimuthal and vertical coordinates r, θ and z (figure 4.1) and corresponding velocities $u = dr/dt$, $v = r\,d\theta/dt$ and $w = dz/dt$. For inviscid, homogeneous flow, the equations are

$$\frac{1}{r}\frac{\partial}{\partial r}ru + \frac{1}{r}\frac{\partial v}{\partial \theta} + \frac{\partial w}{\partial z} = 0. \tag{4.0.1}$$

$$\frac{Du}{Dt} = \frac{v^2}{r} - \frac{\partial \pi}{\partial r} \tag{4.0.2}$$

$$\frac{Dv}{Dt} = -\frac{uv}{r} - \frac{1}{r}\frac{\partial \pi}{\partial \theta} \tag{4.0.3}$$

$$\frac{Dw}{Dt} = \frac{\partial \pi}{\partial z}, \tag{4.0.4}$$

where the material derivative is

$$\frac{D}{Dt} = \frac{\partial}{\partial t} + u\frac{\partial}{\partial r} + \frac{v}{r}\frac{\partial}{\partial \theta} + w\frac{\partial v}{\partial z}. \tag{4.0.5}$$

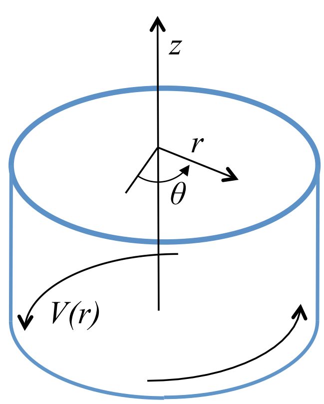

Figure 4.1: Axisymmetric (circular) vortex with cylindrical coordinates.

4.1 Cyclostrophic equilibrium

We now seek an equilibrium state in which the flow is purely azimuthal: $u = 0$, $w = 0$, $v = V(r)$. The divergence equation is satisfied automatically. The momentum equations (4.0.2-4.0.4) become The equations of motion become

$$\begin{aligned} \frac{V^2}{r} &= \frac{\partial \Pi}{\partial r} \\ \frac{\partial \pi}{\partial \theta} &= 0 \\ \frac{\partial \pi}{\partial z} &= 0. \end{aligned}$$

The pressure field can vary only in r, and is related to the azimuthal velocity by

$$\frac{d}{dr}\Pi(r) = \frac{V(r)^2}{r}.$$

This balance between the pressure gradient and the centrifugal force is called cyclostrophic equilibrium.

It is also useful to define the angular velocity:

$$\Omega(r) = \frac{V}{r},$$

the vertical vorticity

$$Z(r) = \frac{1}{r}\frac{d}{dr}rV,$$

and the streamfunction $\Psi(r)$ such that

$$V(r) = -\frac{d\Psi}{dr}.$$

4.2 The perturbation equations

Now imagine a small perturbation to cyclostrophic equilibrium:

$$u = \varepsilon u_r\ ; \quad v = V(r) + \varepsilon v'\ ; \quad w = \varepsilon w'\ ; \quad \pi = \varepsilon \pi'.$$

Substituting into (4.0.1-4.0.4) and linearizing, we obtain at $O(\varepsilon)$:

$$\frac{1}{r}\frac{\partial}{\partial r}ru' + \frac{1}{r}\frac{\partial v'}{\partial \theta} + \frac{\partial w'}{\partial z} = 0. \tag{4.2.1}$$

$$\left[\frac{\partial}{\partial t} + \Omega\frac{\partial}{\partial \theta}\right]u' = 2\Omega v' - \frac{\partial \pi'}{\partial r} \tag{4.2.2}$$

$$\left[\frac{\partial}{\partial t} + \Omega\frac{\partial}{\partial \theta}\right]v' = -Zu' - \frac{1}{r}\frac{\partial \pi'}{\partial \theta} \tag{4.2.3}$$

$$\left[\frac{\partial}{\partial t} + \Omega\frac{\partial}{\partial \theta}\right]w' = -\frac{\partial \pi'}{\partial z}. \tag{4.2.4}$$

Exercise: Fill in the algebra.

Figure 4.2: Barotropic perturbations of a circular vortex, seen in plan view. In all cases $m = 0$.

Since the coefficients of the linearized equations depend on r, we seek a normal mode solution with the r-dependence undetermined:

$$u' = \hat{u}(r)e^{\sigma t}e^{\imath(\ell\theta+mz)},$$

where ℓ is an integer and only the real part is physically relevant. Substituting into the linearized equations (4.2.1-4.2.4) gives

$$\frac{1}{r}(r\hat{u})_r + \frac{\imath\ell}{r}\hat{v} + \imath m\hat{w} = 0. \tag{4.2.5}$$

$$(\sigma+\imath\ell\Omega)\,\hat{u} = 2\Omega\hat{v} - \hat{\pi}_r \tag{4.2.6}$$

$$(\sigma+\imath\ell\Omega)\,\hat{v} = -Z\hat{u} - \frac{\imath\ell}{r}\hat{\pi} \tag{4.2.7}$$

$$(\sigma+\imath\ell\Omega)\,\hat{w} = -\imath m\hat{\pi}. \tag{4.2.8}$$

Two classes of perturbation are important and relatively easy to deal with: barotropic and axisymmetric. A barotropic perturbation has $m = 0$, i.e. no dependence on z. The first-mode barotropic instability has $\ell = 1$ (figure 4.2a), and shifts the entire vortex horizontally. Such instabilities have been suggested as contributors to the motion of hurricanes and tornadoes. Higher-order barotropic modes ($\ell = 2,3,...$, figure 4.2b,c, figure 4.4) leave the vortex in place but distort its circular shape in increasingly ornate ways.

The second important class of disturbances is the axisymmetric modes. These have $\ell = 0$, and hence no dependence on θ, but $m \neq 0$ (figure 4.4a).

In each of these special cases there is a (relatively) easy way to collapse (4.2.5-4.2.5) into a single equation.

4.3 Barotropic modes

For barotropic modes, the trick is to recognize that the perturbation flow is two-dimensional and nondivergent, and can therefore be represented by a streamfunction. We therefore define $\hat{\psi}$ such that

$$\boxed{\hat{u} = \frac{\imath\ell}{r}\hat{\psi}\,; \quad \hat{v} = -\hat{\psi}_r.}$$

Note that, with $m = 0$, (4.2.5) is satisfied exactly, and (4.2.8) gives $\hat{w} = 0$. Remaining are two equations for the two unknowns $\hat{\psi}$ and $\hat{\pi}$. These combine to form

$$\boxed{(\sigma+\imath\ell\Omega)\left[(r\hat{\psi}_r)_r - \frac{\ell^2}{r}\hat{\psi}\right] = \imath\ell Z_r\hat{\psi}.} \tag{4.3.1}$$

Exercise: Show this.

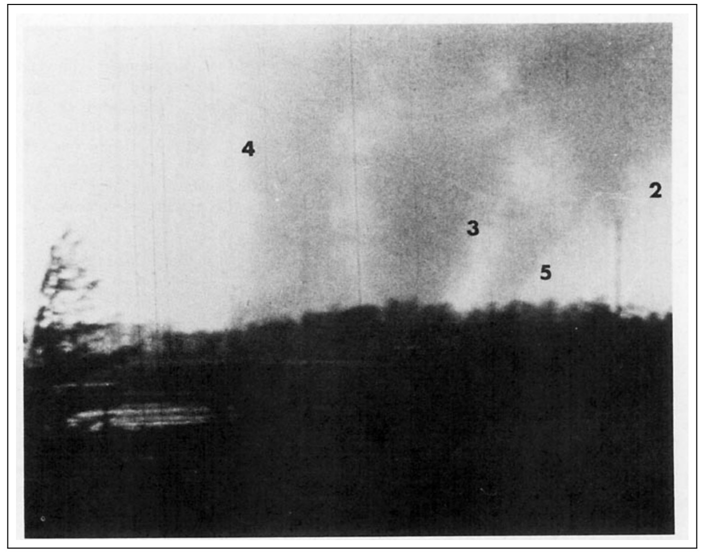

Figure 4.3: Secondary vortices in a tornado suggestive of barotropic instability. (W. Hubbard, WISH Indianapolis; Snow 1978).

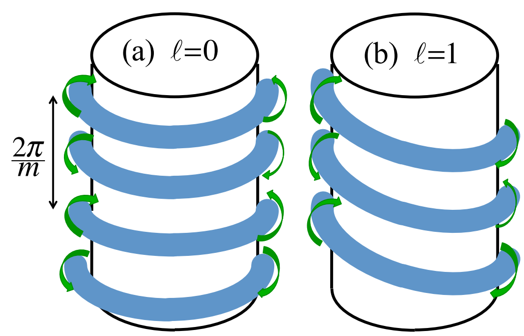

Figure 4.4: (a) Axisymmetric perturbation of a circular vortex. The mode takes the form of counterrotating secondary vortices. (b) General, normal mode perturbation. In this case $\ell = 1$.

4.3.1 Boundary conditions for barotropic modes

- An impermeable boundary can be placed at any radius, say $r = r_1$. Impermeability requires that the radial velocity be zero at that boundary: $\hat{u} = 0$ of, assuming $\ell \neq 0$,

$$\hat{\psi}(r_1) = 0.$$

- If the inner boundary is to be placed at $r = 0$, then we need an approximate solution for (4.3.1) that becomes exact as $r \to 0$. Suppose that $\hat{\psi}$ is proportional to r^α. Substituting into (4.3.1) and multiplying through by $r^{1-\alpha}$, we get

$$(\sigma + \imath\ell\Omega)(\alpha^2 - \ell^2) = \imath\ell Z_r \hat{\psi}\, r. \tag{4.3.2}$$

  We haven't specified the background profiles $\Omega(r)$ and $Z(r)$, but as long as Z is finite then the right-hand size goes to zero as $r \to 0$, and therefore as long as $\sigma - \imath\ell\Omega \neq 0$ then $\alpha^2 - \ell^2 = 0$. Choosing the solution that's bounded as $r \to 0$, we have

$$\hat{\psi} \propto r^\ell \,, \quad \text{or } \hat{\psi}(0) = 0.$$

  In numerical calculations it is not a problem to have the inner boundary at $r = 0$, even though r appears in the denominator of (4.3.1). This is because $r_0 = 0$ is a ghost point, so nothing is ever actually evaluated there.

- If the outer boundary is at infinity, we can again assume that $\hat{\psi} \propto r^\alpha$, resulting in (4.3.3). If we now assume that Z_r decays to zero faster than $1/r$ as $r \to \infty$, then the right-hand side goes to zero, and if $\sigma - \imath\ell\Omega \neq 0$ we again have $\alpha = \pm\ell$. The bounded solution is now

$$\hat{\psi} \propto r^{-\ell} \,, \quad \text{or } \lim_{r\to\infty} \hat{\psi}(r) = 0.$$

- In numerical calculations, we can't actually place the outer boundary at infinity, so we place it at some large but finite radius (hopefully where Z_r has decreased almost to zero) and apply the asymptotic condition

$$\hat{\psi}_r = -\ell\hat{\psi}.$$

  The perturbation equation (4.3.1) can then be reduced to a generalized eigenvalue problem using derivative matrices as in the case of parallel flows.

The numerical solution of (4.3.1) just as we did with the parallel shear flow. We first replace the derivatives with derivative matrices incorporating the appropriate boundary conditions. We then arrange the equation as an eigenvalue equation and find the eigenvalues and eigenvectors numerically.

Admonition: It may be tempting to define a first derivative matrix $\underset{\sim}{D}^{(1)}$, then use it twice to form the second derivative. Don't do this - it effectively replaces the grid spacing Δ by 2Δ, degrading the accuracy of the results. In (4.3.1), the first term in the brackets should be computed in the expanded form

$$\underset{\sim}{D}^{(1)} + r \cdot \underset{\sim}{D}^{(2)},$$

rather than the simpler but less accurate

$$\underset{\sim}{D}^{(1)} r \cdot \underset{\sim}{D}^{(1)}.$$

4.3.2 Stability theorem for barotropic modes

We rewrite (4.3.1) as

$$(r\hat{\psi}_r)_r - \frac{\ell^2}{r}\hat{\psi} = \frac{\imath\ell Z_r\hat{\psi}}{\sigma+\imath\ell\Omega}, \tag{4.3.3}$$

then apply the operator $\int_{r_1}^{r_2}\hat{\psi}^* dr$. The radii r_1 and r_2 are the boundaries of the domain. The inner boundary radius may be $r_1 = 0$, and the outer may be $r_2 = \infty$.

The first term on the left gives

$$\int_{r_1}^{r_2}\hat{\psi}^*(r\hat{\psi}_r)_r\,dr \;=\; \hat{\psi}^* r\hat{\psi}_r\Big|_{r_1}^{r_2} \;-\; \int_{r_1}^{r_2} r|\hat{\psi}|^2\,dr$$

Using the boundary conditions derived in the previous subsection, the first term vanishes, leaving

$$\int_{r_1}^{r_2}\hat{\psi}^*(r\hat{\psi}_r)_r\,dr \;=\; -\int_{r_1}^{r_2} r|\hat{\psi}|^2\,dr$$

The second term on the left is just

$$\int_{r_1}^{r_2}\frac{\ell^2}{r}|\hat{\psi}|^2 dr.$$

Note that both of the above integrals are real. Applying the integral operator to the right-hand side and taking the imaginary part, we have

$$0 = \Im\int_{r_1}^{r_2}\frac{\imath\ell Z_r}{\sigma+\imath\ell\Omega}\,|\hat{\psi}|^2 dr$$

Multiplying and dividing the integrand by the complex conjugate $\sigma^* - \imath\ell\Omega$ gives

$$0 = \Im\int_{r_1}^{r_2}\frac{\imath\ell Z_r}{|\sigma+\imath\ell\Omega|^2}\,(\sigma^*-\imath\ell\Omega)\,|\hat{\psi}|^2 dr = \ell\sigma_r\int_{r_1}^{r_2}\frac{Z_r|\hat{\psi}|^2}{|\sigma+\imath\ell\Omega|^2}dr.$$

For a growing (or decaying) mode, $\sigma_r \neq 0$, and therefore the integral must vanish, i.e. Z_r must change sign at least once in $r_1 < r < r_2$.

> *Theorem:* Given an inviscid, homogeneous, circular vortex, a necessary condition for barotropic instability is that the vorticity gradient $Z_r(r)$ change sign somewhere in the domain $r_1 < r < r_2$.

4.4 Axisymmetric modes

In the axisymmetric case $\ell = 0$, (4.2.5-4.2.5) can be combined into a single equation for the radial velocity perturbation $\hat{u}$:

$$\boxed{\sigma^2\left\{\left[\frac{1}{r}(r\hat{u})_r\right]_r - m^2\hat{u}\right\} = m^2\Phi\hat{u},} \tag{4.4.1}$$

where

$$\Phi(r) = 2\Omega Z$$

is called the Rayleigh discriminant.

4.4.1 Boundary conditions for axisymmetric modes

- If an impermeable boundary is placed at some r_1, then the radial velocity must vanish there, i.e. the boundary condition is just $\hat{u}(r_1) = 0$.

- Now suppose there is no inner boundary, so we need a virtual boundary condition at $r = 0$. Assume that, for r near zero, $\hat{u}$ is proportional to r^α. Substituting into (4.4.1) and multiplying through by $r^{2-\alpha}$, we obtain
$$\sigma^2\{\alpha^2 - 1 - m^2r^2\} = m^2r^2\Phi.$$
Assuming that Φ remains finite, the right-hand side must vanish as $r \to 0$. Therefore, for nonzero σ, the quantity in braces must vanish as $r \to 0$ and $\alpha = \pm 1$. To keep the solution bounded, we choose $\alpha = 1$, i.e. $\hat{u} \propto r$. The boundary condition at $r = 0$ is therefore
$$\hat{u}(0) = 0.$$

- If there is no outer boundary, we employ an asymptotic boundary condition. We will assume that the vortex is *isolated*, meaning that if you go far enough away, the vortex motion vanishes. More specifically, $\Phi \to 0$ as $r \to \infty$. In that case, for sufficiently large r, (4.4.1) becomes
$$\left[\frac{1}{r}(r\hat{u})_r\right]_r - m^2\hat{u} = 0$$
This is the *modified Bessel equation*, and its bounded solution is the first-order modified Bessel function:
$$\hat{u} = K_1(mr).$$
As $r \to \infty$, K_1 can be approximated using Stirling's formula
$$K_1(mr) \approx \frac{e^{-mr}}{\sqrt{2\pi mr}}; \quad \text{for } mr \gg 1.$$
Therefore, $\hat{u} \to 0$ in the limit $r \to \infty$.

- An asymptotic condition is also available for use in numerical calculations where the domain must be finite. Taking the logarithmic derivative of the Stirling approximation to K_1,
$$\frac{\hat{u}_r}{\hat{u}} = (\ln\hat{u})_r \;=\; \left[-mr - \frac{1}{2}\ln(2\pi mr)\right]_r = -m - \frac{1}{2r}.$$
So if the computation domain ends at $r = R$, the asymptotic boundary condition is
$$\hat{u}_r = -\left(m + \frac{1}{2R}\right)\hat{u}.$$

4.4.2 Stability theorem for axisymmetric modes

We now apply the integral operator $\int_{r_1}^{r_2} dr\, r\hat{u}^*$ to (4.4.1). Here, r_1 and r_2 are the boundaries of the domain. The inner boundary radius may be $r_1 = 0$, and the outer may be $r_2 = \infty$. We'll apply this operator individually to the two terms on the left-hand side and the single term on the right. The first term on the left, omitting the factor σ^2 for now, gives

$$\begin{aligned}\int_{r_1}^{r_2} r\,\hat{u}^*\left[\frac{1}{r}(r\hat{u})_r\right]_r dr &= \hat{u}^*(r\hat{u})_r\Big|_{r_1}^{r_2} - \int_{r_1}^{r_2}(r\hat{u}^*)_r\,\frac{1}{r}\,(r\hat{u})_r dr\\ &= -\int_{r_1}^{r_2}\frac{dr}{r}\left|(r\hat{u})_r\right|^2.\end{aligned}$$

Here, the boundary conditions derived in the previous subsection have been used. The second term (without the factor $-\sigma^2 m^2$) is

$$\int_{r_1}^{r_2} r\,\hat{u}^*\hat{u}dr = \int_{r_1}^{r_2} r\,\left|\hat{u}\right|^2 dr.$$

Finally, the right-hand side (omitting m^2) is

$$\int_{r_1}^{r_2} r\,\Phi\left|\hat{u}\right|^2 dr.$$

Combining these results and restoring the various constants, we have

$$\sigma^2\left\{\int_{r_1}^{r_2}\frac{dr}{r}\left|(r\hat{u})_r\right|^2 + m^2\int_{r_1}^{r_2} r\,\left|\hat{u}\right|^2 dr\right\} = -m^2\int_{r_1}^{r_2} r\,\Phi\left|\hat{u}\right|^2 dr$$

or, with some rearranging

$$\sigma^2\int_{r_1}^{r_2}\frac{dr}{r}\left|(r\hat{u})_r\right|^2 = -m^2\int_{r_1}^{r_2} r\,\left|\hat{u}\right|^2(\sigma^2+\Phi)\,dr. \tag{4.4.2}$$

For $\sigma^2 > 0$ the final integral must be negative, and therefore $\sigma^2+\Phi$ must be negative for some r. Therefore the minimum value of $\Phi(r)$ must be less than $-\sigma^2$. If we call that minimum value Φ_{min}, then

$$\sigma < \sqrt{-\Phi_{min}}. \tag{4.4.3}$$

Instability is possible provided that $\Phi_{min} < 0$. This class of unstable modes is called centrifugal instability.

> Theorem: Given an inviscid, homogeneous, circular vortex, a necessary and sufficient condition for centrifugal instability is that the Rayleigh discriminant $\Phi(r) = 2\Omega(r)Z(r)$ be negative for some r. Moreover, (4.4.3) gives an upper bound on the growth rate.

In a sense, centrifugal instability is analogous to convection. In the convective case, if $B_z < 0$, the fluid possesses gravitational potential energy that can be converted to kinetic energy. Here, a variant of potential energy due to the centrifugal force is available for conversion to kinetic energy wherever $\Phi < 0$.

4.5 Example 1: the Rankine vortex

The Rankine vortex has uniform vorticity inside a radius R and zero vorticity outside (figure 4.5, black curves). There is no radius at which the vorticity gradient changes sign, so there is no possibility of barotropic instability. How about centrifugal instability? The azimuthal velocity profile is:

$$V(r) = \begin{cases}\Omega_0 r\,, & \text{for } r \le R\\ \Omega_0\dfrac{R^2}{r}\,, & \text{for } r \ge R\end{cases} \quad\Rightarrow\quad \Phi(r) = \begin{cases}4\Omega_0^2\,, & \text{for } r \le R\\ 0\,, & \text{for } r \ge R\end{cases}. \tag{4.5.1}$$

With no negative values of Φ, there can be no centrifugal instability.

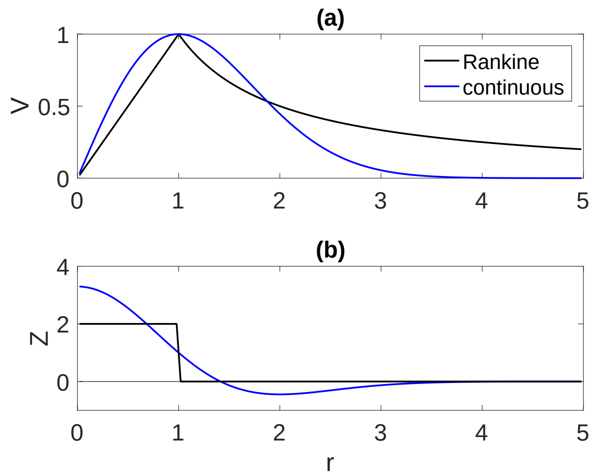

Figure 4.5: Profiles of velocity (a) and vorticity (b) for the Rankine vortex (4.5.1) with $\Omega_0 = R = 1$ and the continuous vortex (4.6.1).

4.6 Example 2: A continuous vortex

A vortex with continuous profiles, scaled so that the maximum flow and the radius of maximum flow are both unity (figure 4.5, blue curves), can be modeled as:

$$V = r\,e^{-\frac{1}{2}(r^2-1)}\ ; \quad Z = (2-r^2)\,e^{-\frac{1}{2}(r^2-1)}. \tag{4.6.1}$$

4.6.1 Barotropic modes

Because the vorticity gradient changes sign at $r = 2$, barotropic instability is possible (section 4.3.2).

In fact, the barotropic mode with $\ell = 2$ is unstable as shown in figure **??**a. The streamfunction eigenfunction has maximum amplitude just inside $r = 2$, the inflectional radius, and the phase shifts rapidly near this radius. The sign of the phase shift is such that phase lines of the radial velocity tilt against the vorticity. This is the circular analog of the instability of a parallel shear flow (chapter 3).

The velocity perturbation causes the vortex to bulge inward and outward as in figure 4.2b. The mode is not stationary; it precesses around the vortex with azimuthal velocity about 1/5 that of the maximum flow speed (figure 4.6b).

4.6.2 Axisymmetric modes

The Rayleigh discriminant $2\Omega Z$ is negative for $r > \sqrt{2}$ (where $Z < 0$, figure 4.5b). We therefore expect to find axisymmetric instability, and that expectation is confirmed in the numerical results (figure 4.8). There is no preferred vertical scale: the growth rate increases monotonically with increasing vertical wavenumber. This is the phenomenon of ultraviolet catastrophe, as we found previously with convective instability of an inviscid fluid (section 2.3). As $m \to \infty$, the growth rate approaches the maximum value $\sqrt{-\Phi_{min}}$.

The radial velocity is greatest near $r = \sqrt{3}$, where Φ is most negative. As m is increased, the eigenfunction becomes more tightly concentrated near that radius. The result is a stack of counter-rotating vortices

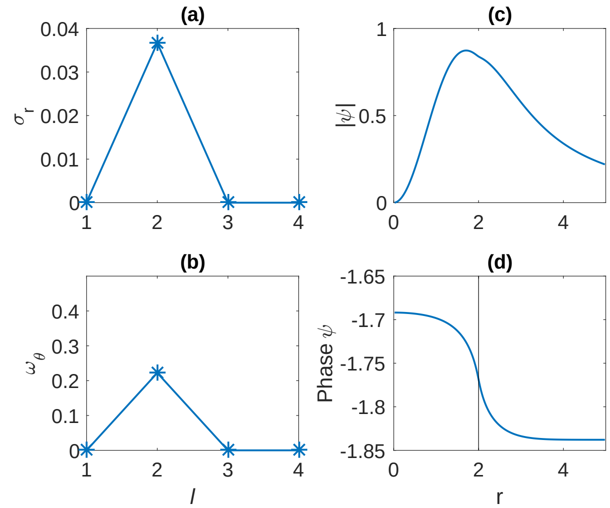

Figure 4.6: Growth rate (a) and frequency (b) versus azimuthal wavenumber for barotropic modes. Amplitude (c) and phase (d) profiles for the fastest-growing barotropic mode. Vertical line shows the radius of minimum vorticity (cf. figure 4.5).

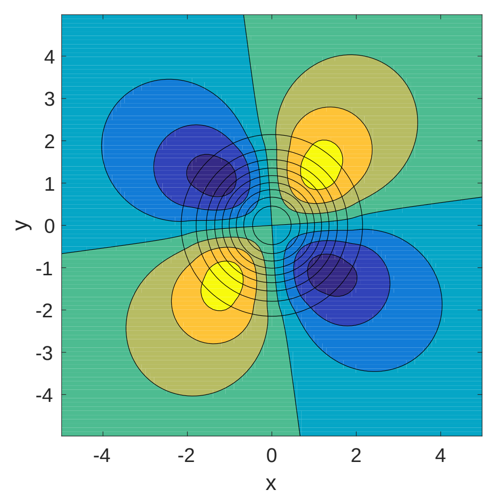

Figure 4.7: Stream function for the fastest-grow barotropic mode. Circles are streamlines of the ba ground flow.

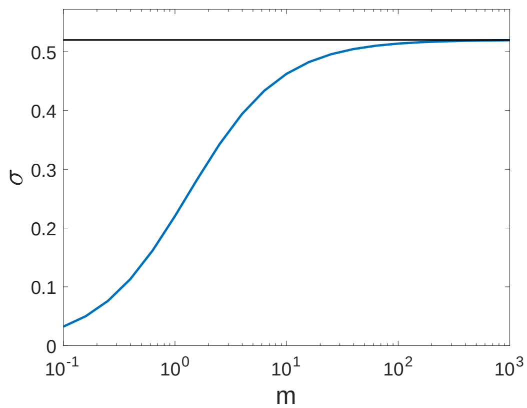

Figure 4.8: Growth rate versus vertical wavenumber for axisymmetric modes. Black line shows Rayleigh's upper bound $\sqrt{-\Phi_{min}}$.

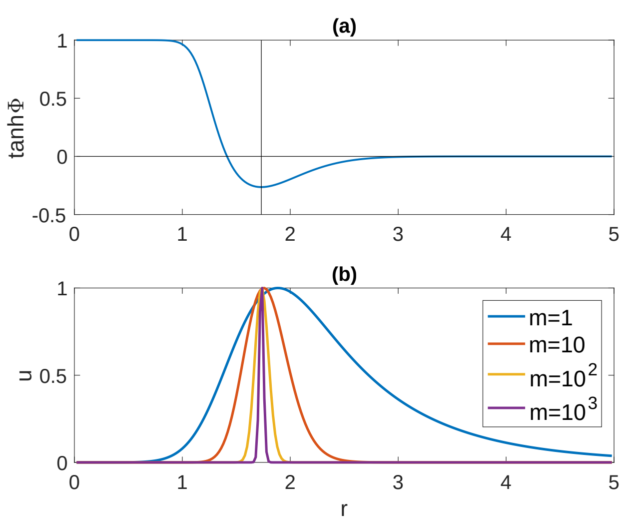

Figure 4.9: (a) Profile of the Rayleigh discriminant $\Phi = 2\Omega Z$, scaled using the tanh function to make the minimum visible. The vertical line indicates $r = \sqrt{3}$, where Φ is a minimum. (b) Eigenfunction of the radial velocity for various m.

surrounding the background vortex, as sketched in figure 4.4a.

4.7 Further reading

Drazin, P.G. and W.H. Reid, 1981: *Hydrodynamic stability*, Cambridge University Press.

This classic text contains an extensive discussion of vortex instabilities.

Kundu, P.J., I.M. Cohen and D.R. Dowling, 2016: *Fluid Mechanics, 6th ed.*, Academic Press.

Among many other useful features, this excellent reference monograph has an appendix that gives the equations of motion in cylindrical and other curvilinear coordinate systems.